Windowed Correlated Kurtosis for Isolation and Identification of Compound Faults in Locomotive Bearings

Jianxiang Xu, Chunlin Zhang*, Fangyi Wan
School of Aeronautics
Northwestern Polytechnical Universtiy
Xi'an, Shanxi 710072, P.R. China
*Corresponding Author: zchunlin@nwpu.edu.cn (CZ)

Jie Liu[1, 2]
[1]School of Aeronautics, Northwestern Polytechnical University, Xi'an, Shaanxi, 710072, P.R. China
[2]Department of Mechanical and Aerospace Engineering, Carleton University, Ottawa, ON K1S5B6, Canada

***Abstract*—Compound faults commonly occur on the rolling bearings. The faults isolation and identification of locomotive bearings are significantly important for bearing health management while difficult in engineering applications. In this paper, a method termed windowed correlated kurtosis (WCK) is presented to successively isolate each impulsive fault mode from compound-fault signals and identify the defects number. To apply WCK for analyzing noise-rich, experiment measurements, a technique frame is proposed which mainly contains two steps: frequency filtering; and WCK based faults isolation. During the filtering procedure, flexible wavelet frames such as tunable Q-factor wavelet transform and flexible analytical wavelet transform which possess arbitrary time-frequency partition property are suggested to adaptively filter the raw vibration measurements such that the signal-to-noise ratio could be enhanced in the filtered signal. Further, WCK is conducted on the filtered signal. The fault modes will be successively isolated in the WCK outputs and the fault signature would be captured on the envelope spectrum. The effectiveness of the proposed technique is validated via analysis of experimental data measured from damaged locomotive bearings subjected to multiple defects on the outer race and roller elements.**

Keywords-compound faults diagnosis; locomotive bearings; windowed correlated kurtosis; fault impulses isolation; flexible analytical wavelet transform

I. INTRODUCTION

Rolling bearings are the primary supporting structures in electric locomotives, and may suffer local damages under heavy and fatigue loads. Operation status monitoring and health management of locomotive rolling bearings are significantly important to prevent potential failures and provide adequate early warning and maintenance time [1-3].

Based on the dynamics and fault mechanism of roller bearings [4], the fault features are a set of periodic, impulsive vibration responses. To date, a lot of research work has been conducted on detecting single damage for rolling bearings, and many vibration data driven approaches have been reported [5-7]. Most of these detection methods follow the denoising principle of improving the signal-to-noise ratio (SNR), and the fault signature is further captured as the fundamental and harmonics of the fault characteristic frequency. Though fruitful achievements have been reported on diagnosing single damage, compound faults isolation and diagnosis of locomotive bearings are still difficult. Based on the fault mechanism, the periodic fault impulses are essentially similar with the dynamic responses of impact modal test. Though the contact positions of the local defects with contacted components vary during the rotation, the frequency spectrum of the compound-fault induced impulses are always close to the resonant frequency of the rolling bearing system. Thus, the direct adoption of filtering based methods fails to diagnosis the compound faults especially when one of the faults is weaker than others.

To date, compound faults detection has drawn increased attention. Miao et al. proposed a maximum correlated kurtosis deconvolution method [8]. Wang et al. [9] combined the blind source separation and ensemble empirical mode decomposition methods for compound faults diagnosis. Hao et al. [10] proposed sparsity promoted-based sparse component analysis for diagnosis of compound faults. Besides, some other approaches are proposed for diagnosing the compound faults of rotating machinery, such as wavelet transform approach [11-15], minimum entropy deconvolution [16], and blind deconvolution algorithm [17]. Most of these methods focus on enhancing the SNR of interested fault mode from the denoised signals which are still company with certain-lever noise and other fault modes. Thus, the effectiveness of these methods will be weakened when detecting weak transient faults from noise-rich, compound-faults signals or when estimating the defects number when multiple defects occur in the same bearing component such as multiple damages on the rollers (i.e., the compound transient faults share common resonant frequency as well as common fault characteristic frequency).

In this paper, a novel concept of windowed correlated kurtosis (WCK) is adopted for diagnosing the compound faults. WCK essentially calculates the correlation coefficient of the filtered signal with the interested fault mode as the interval. Thus, WCK would effectively enhance the periodicity

This study was financially supported in part by the Fundamental Research Funds for the Central Universities grant 310201901A009, and China Postdoctoral Science Foundation grant 2018M631196.

978-1-7281-0860-5/19/$31.00 ©2019 IEEE

components and eliminate the noise and unwanted vibrations. Each interested fault mode (i.e., transient faults possessing the interested fault period) could be successively isolated from the compound faults, and the damages number is further determined via evaluating the sets number of the periodic pulses in the WCK outputs. To analyze the noise-rich vibration signals from engineering experiments, a technique frame is proposed which mainly contains two steps: filtering procedure; and WCK isolation procedure.

The structures of this paper are organized as follows. The WCK is defined in Section 2, and its ability in isolating and identifying compound faults is also numerically tested. The advantages and disadvantages of the WCK are also explained in this section. The proposed compound fault identification procedures are given here. The performance of the proposed method is tested via analyzing vibration measurements from damaged locomotive bearings subjected to two local defects on the rollers and three outer race damages in Section 3. Finally, Section 4 remarks the main conclusions.

II. WINDOWED CORRELATED KURTOSIS (WCK)

A. Definition of WCK

The windowed correlated kurtosis (WCK) is inspired by the correlated kurtosis (CK). CK was for the first time proposed by McDonald et al [18]. For a tested signal $_1$, the CK is given as:

$$CK_M\left(T_s\right)=\frac{\sum_{n=1}^{N}\left(\prod_{m=0}^{M} y_{n-mT_s}\right)^2}{\left(\sum_{n=1}^{N} y_n^2\right)^{M+1}} \tag{1}$$

in which M is the shift order and is positive integer; and $T_s = f_s \cdot T$ is sampling point of the interested periodic fault impulses where f_s denotes the sampling frequency of the discrete signal and T presents the period of interested fault mode. The CK has been validated to be more effective as an index than kurtosis in denoting periodic fault impulses instead of a single impulse. Moreover, with artificial set of T_s, the CK exhibits great advantage in revealing the richness of interested fault impulses with pre-evaluated period.

Inspired by the short-time Fourier transform (STFT) where the windowing operation enables STFT to analyze the instantaneous time-frequency information of the nonstationary signals, the WCK is supposed to identify the occurrence moments of interested fault and is defined as:

$$WCK_{M,W}\left(n,T_s\right)=\frac{\sum_{n}^{n+(W-M)T_s}\left(\prod_{m=0}^{M} y_{n-mT_s}\right)^2}{\left(\sum_{n}^{n+WT_s} y_n^2\right)^{M+1}} \tag{2}$$

where $n=1,2,\cdots,N$, $T_w = W \cdot T_s$ is the window width; W satisfies $W \geq M$ and is termed as the order of the window width. Specifically, when $W = M$, the WCK is simplified to be:

$$WCK_M\left(n,T_s\right)=\frac{\left(\prod_{m=0}^{M} y_{n-mT_s}\right)^2}{\left(\sum_{n}^{n+WT_s} y_n^2\right)^{M+1}} \tag{3}$$

Equation (3) mathematically evaluates the correlation coefficient of local points staring from y_n with the interval of T_s, and outputs large if y_n locates at any peak of the periodic impulses; while Equation (2) also considers the starting points around y_n which may average and weaken the characterization performance of fault impulses at y_n. Accordingly, the WCK is hereafter defined as (3) in this paper where the default order of the window width is $W = M$.

B. Numerical Example of WCK in Isolating Compound Impulsive Faults

Based on the fault mechanism, a series of successive impulses are widely adopted to describe the produced signal from bearing defects. The amplitudes of the impulses are modulated by the shaft rotating speed and bearing geometry parameters, and can be expressed as:

$$\begin{aligned} x_1(t) &= \sum_{i=1,2,\ldots}\left(\cos\left(2\pi f_{r1}t\right)+1\right)\left[a_1 e^{-\zeta\left(t-iT_1\right)}\cdot\cos\left(2\pi f_{n1}\left(t-iT_1\right)\right)\right] \\ &+ \sum_{i=1,2,\ldots}\left(\cos\left(2\pi f_{r2}t\right)+1\right)\left[a_2 e^{-\zeta\left(t-iT_2\right)}\cdot\cos\left(2\pi f_{n1}\left(t-iT_2\right)\right)\right]+n(t) \end{aligned} \tag{4}$$

in which, $x_1(t)$ considers two sets of periodic impulses whose periods are respectively T_1 and T_2 . a_1 and a_2 are the peak amplitudes of the impulsive responses which oscillate in the resonant frequency f_{n1} with the decaying rate denoted by the damping coefficient ζ ; f_{r1} and f_{r2} are modulation frequencies of the impulse amplitudes and simulate the amplitude modulation in inner and roller defects; and $n(t)$ is the noise. Table 1 lists the parameter values of the signal $x_1(t)$. Considering the focus here is to illustrate the principle of WCK in isolating different faults, only the noise-free signal is analyzed in this part. Fig. 1(b) shows the waveforms of the simulated signals using solid line (gray) with $f_s = 10\text{kHz}$.

TABLE I. THE PARAMETERS OF THE SIMULATED SIGNAL

$1/T_1$	$1/T_2$	f_{n1}	f_{r1}	f_{r2}	a_1	a_2	ζ
16	20	550	51	23	1	1	330

The sampling points during one fault period for the two interested fault modes are estimated as $T_{s1} = f_s \cdot T_1 = 625$ and $T_{s2} = 500$, respectively. Via calculating the CK values of the

whole signal $x_1(t)$ based on (1) under varied shift order M, it is found $M=1$ leads to maximal outputs for both $CK_M(T_{s1})$ and $CK_M(T_{s2})$. Thus, the optimal shift and window orders are chosen as $W=M=1$. Recalling (3), the windowed CK values, ie., $WCK_1(t,T_{s1})$ and $WCK_1(t,T_{s2})$, are then evaluated and shown in Fig. 1(a) and (c), respectively.

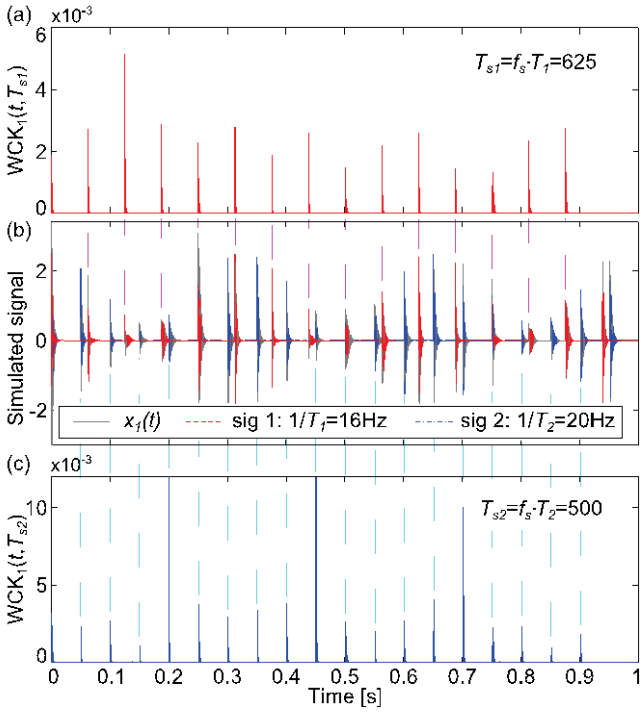

Figure 1. Simulated signals and the WCK values: (a) $\mathrm{WCK}_1(t,T_{s1})$ based on T_1; (b) simulated signals (in gray) which contains two sets of periodic impulses whose periods are respectively $T_1=1/16$s for the dashed (red) curves and $T_2=1/20$s for the dotted (blue) curves; and (c) $\mathrm{WCK}_1(t,T_{s2})$ based on T_2.

From Fig. 1, it is revealed that $WCK_1(t,T_{si}), i=1,2$ outputs large-amplitude pulses at the occurrence moments of each set of fault impulses with the period T_{si} while outputs little even null elsewhere, leading to the two functions of WCK: first, the occurrence moments are isolated and indicated by WCK for the interested fault impulses; second, WCK leads to a pure set of period pulses, and the fault signature can be easily observed from the Hilbert envelope spectrum of the WCK outputs, as displayed in Fig. 2 where the Hilbert envelope spectra of the signals in Fig. 1(a) and (c) are obtained.

C. *Pros and Cons of WCK*

(1) Pros: WCK isolates and indicates the occurrence moments of interested periodic fault impulses from compound faults or when the interested fault impulses are mixed with unrelated or random impulses; moreover, WCK outputs a pure set of periodic pulses with the interval equals the period of interested fault impulses, and its envelope spectrum will thus exhibit the isolated signature of the interested fault. The above features of WCK are helpful in engineering applications where the relatively weak fault features are buried in the compound faults and couldn't be well isolated via wavelet-based filtering methods.

(2) Cons: WCK is a time-domain processing technique and only works effectively when the compound fault impulses are primary in the noisy signals. Thus, WCK fails to directly analyze the vibration measurements in which the fault impulses are always strongly polluted by unrelated vibrations and background noise. In the whole route of the proposed technique for fault identification, WCK is a postprocessing procedure for isolating and identifying the interested fault from filtered signals, before which the original vibration measurements are filtered via flexible time-frequency analysis frame such that the SNR of the fault information will be improved.

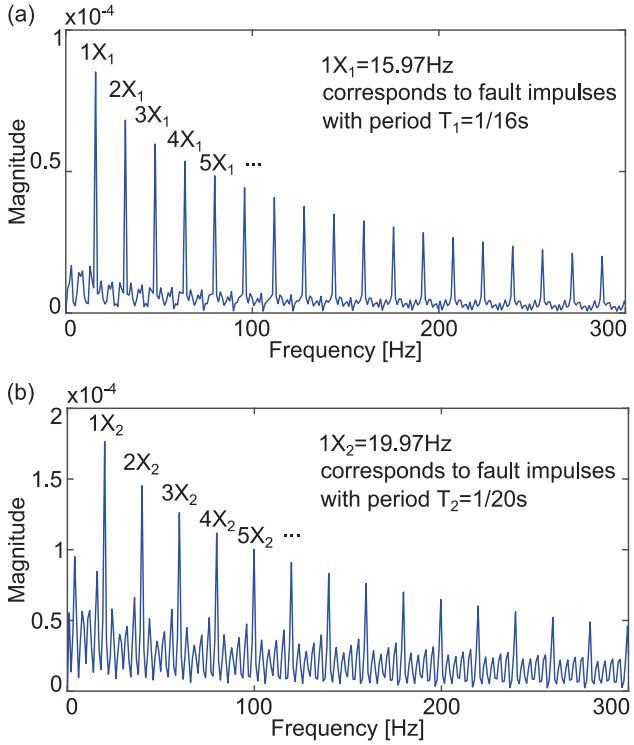

Figure 2. The envelope spectrum analyzed from the WCK signals including (a) $WCK_1(t,T_{s1})$ and (b) $WCK_1(t,T_{s2})$.

D. *Compound Faults Isolation and Identification Procedure*

The proposed technique mainly contains two steps: first, the original vibration measurements are filtered based on flexible wavelet transform frames such as TQWT and FAWT such that to improve the SNR in the filtered signal; second, WCK is then used to successively isolate each interested fault impulses. The main steps are summarized below.

(1) For monitored roller bearings, the common fault modes include outer-race, roller element, and inner-race defects. For each fault mode, the fault characteristic frequencies of each bearing components and T_s need to be estimated before the diagnosis.

(2) Constructing the proper wavelet bases and obtaining the denoised signal possessing the highest signal-to-noise ratio (SNR) of the periodic impulses. FAWT employs fractional and tunable translation and scaling parameters, resulting to arbitrary, tunable time-frequency partition manner for adaptively filtering the vibration signals. The optimized FAWT basis is constructed based on the optimized scaling and translation factors selected from the candidate space. Then the vibration signal is decomposed into subbands via the constructed FAWT basis and the correlated kurtosis is estimated for each filtered subband signal. The filtered signal is selected as the subband possessing the maximal correlated kurtosis.

(3) This step is interested fault mode isolation and identification. The WCK is calculated to isolate the interested fault impulses, and its Hilbert envelope spectrum is further estimated to capture the fault signature.

III. Engineering Validation

The proposed method is tested on compound faults isolation and identification of rolling bearings working at the running part of the high-speed locomotives. As shown in Fig. 3, the tested bearings are double row tapered roller bearings and mounted in the wheelset which is the key supporting and braking component of the locomotive. A triaxial strain gauge accelerometer typed ZW9609A-18SN7068 and a monoaxial piezoelectric accelerometer typed SNY563 are fixed on the bearing house to measure the structure vibrations in all directions. The vibration responses are further recorded via data acquisition with the sampling frequency chosen as 10kHz. In the experiment, the speed of the locomotive remains constantly as 100km/h, and the corresponding shaft rotating frequency is measured as 10.2813Hz. Based on the shaft speed and geometry parameters of the tapered roller bearings, the fault characteristic frequencies corresponding to each bearing structural component are then evaluated and listed in Table II.

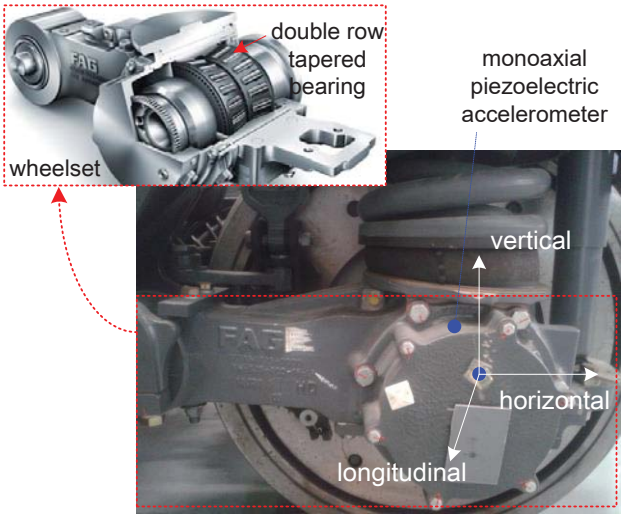

Figure 3. Experiments are conducted on locomotive tapered rolling bearings via measuring the structural vibrations.

TABLE II. Fault Characteristic Frequencies of The Tested Double-row Tapered Roller Bearing

SHAFT	OUTER RACE	INNER RACE	ROLLER
f_r (Hz)	BPFO (Hz)	BPFI (Hz)	BPF=2BSF (Hz)
10.2813	83.2555	112.0888	67.2979

A. Compound Outer Race and Roller Damages

In this case, the method is tested on identifying multiple-components, multiple-location damages in an experimented locomotive bearing. The damages include manually fabricated outer race and roller defects. On the inner surface of the bearing outer race, three localized damages are manually fabricated with the included angle of each two defects equals 120°, as shown in Fig. 4, The sizes of the three outer race damages are separately 1mm, 3mm, and 5mm in width, and commonly 1mm in depth. Two localized damages are fabricated on the surfaces of two rollers. The size of the roller damages is 1mm in the depth and 1mm in the width. The damaged outer race and rollers are in the same row of the double row tapered roller bearing. Theoretically, five sets of impulsive faults are supposed to be occurred in the vibration measurements. In the following analysis, only the vertical vibrations measured at the bearing house by the strain gauge accelerometer is analyzed.

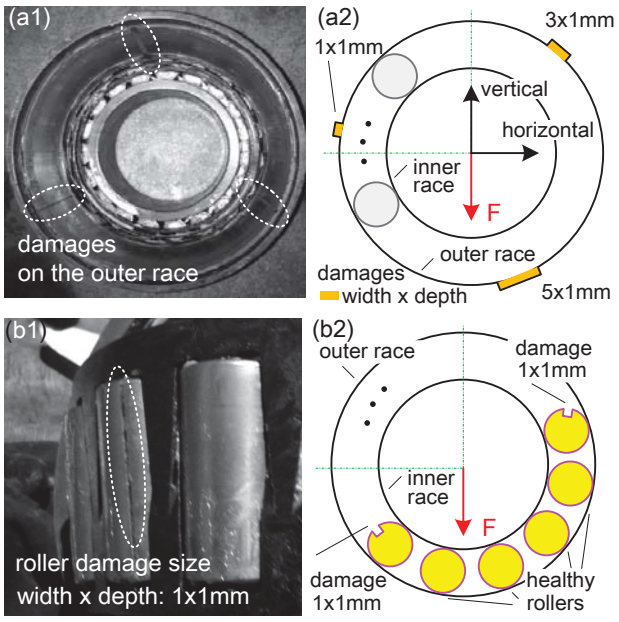

Figure 4. Compound faults on tested locomotive bearing and location illustration: (a1) outer race defects; (a2) locations and sizes of three outer race defects; (b1) roller defects; (b2) locations and sizes of the two roller defects.

B. Experiment Data Analysis

Fig. 5 displays the vibration accelerations lasting for 10 seconds. From Fig. 5, the vibration signals are complicated and periodic, impulsive fault signature are not directly observed even from the zoom-in view. Thus, FAWT based filtering is adopted to obtain high-SNR signals. Following the FAWT basis optimization procedures, the optimized FAWT bases are obtained as: $(p, q, r, s) = (4, 5, 7, 10)$ for detecting the outer race defect; and $(p, q, r, s) = (3, 4, 9, 10)$ for detecting the roller

defect. Via maximizing the FAWT spectrum, the sensitive subband and shift order M are found to be: j=2 and M=1 for $B_{4,5,7,10}$; and j=3 and M=1 for $B_{3,4,9,10}$.

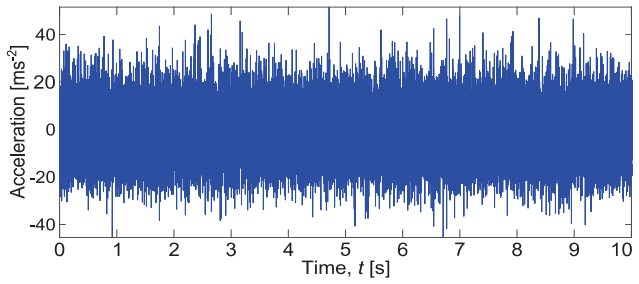

Figure 5. Vibration measurements from multi-damage locomotive bearing.

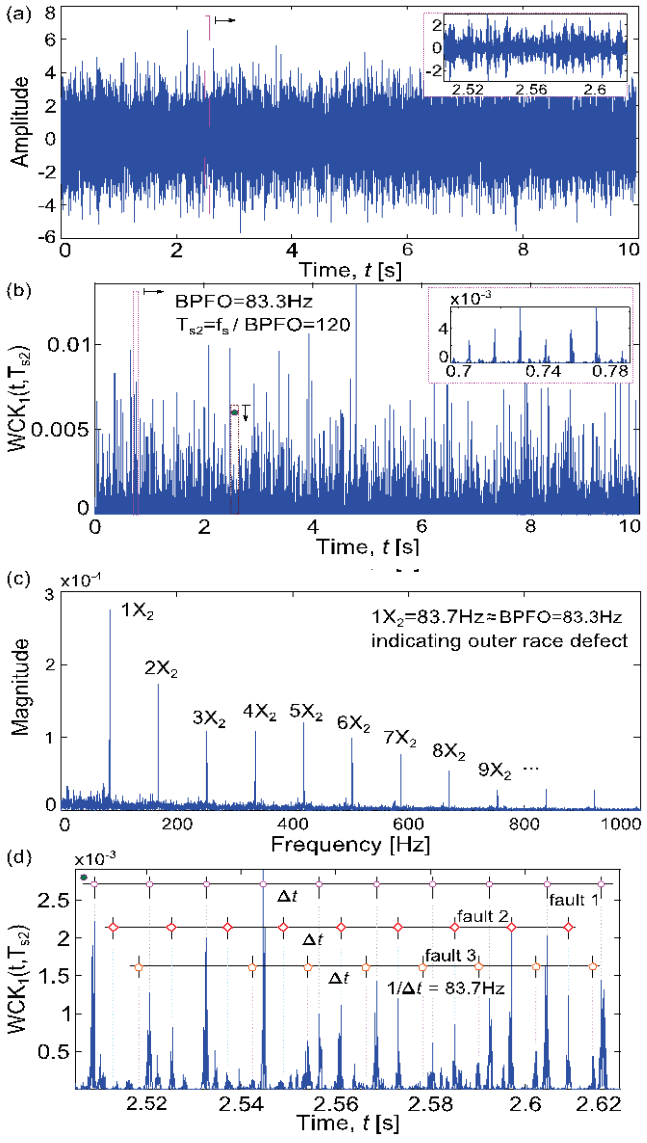

Figure 6. (a) Filtered signal for detecting the outer race detects; (b) WCK; (c) envelope spectrum; and (d) zoom-in view of (b).

Adopting the optimal FAWT basis $B_{4,5,7,10}$ for outer race defect detection, the filtered signal is obtained as the subband signal in the second layer and shown in Fig. 6(a) which exhibits impulsive features.

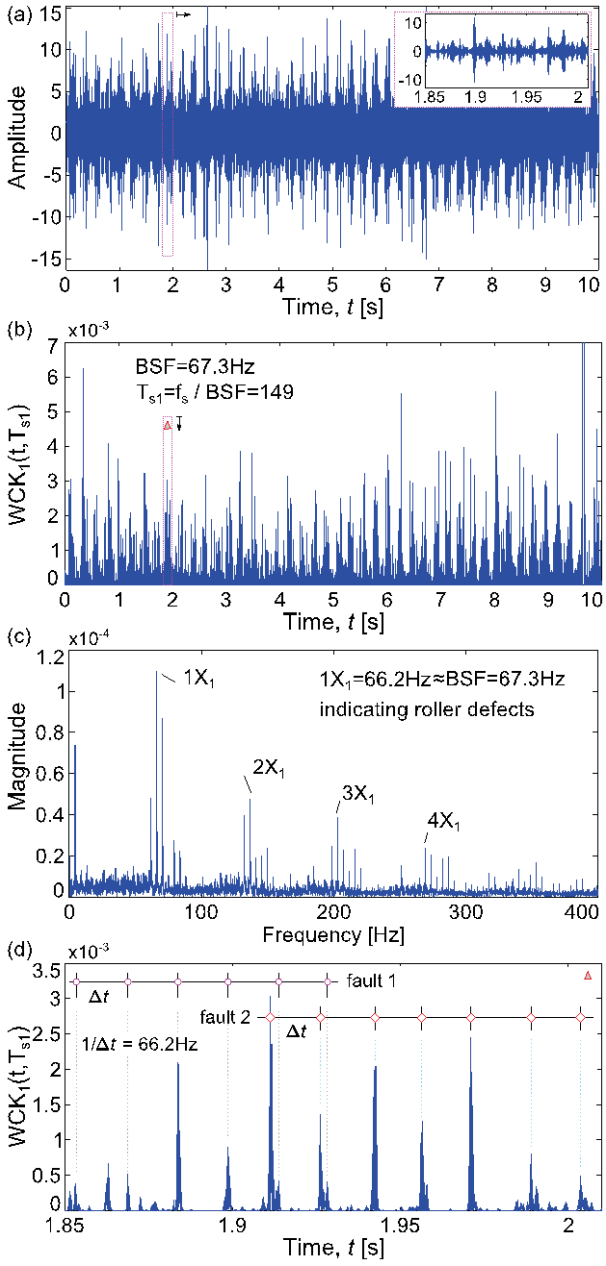

Figure 7. (a) Filtered signal via FAWT basis $B_{3,4,9,10}$ for detecting the roller defect; (b) $WCK_1(t,T_{s1})$ of the filtered signals in (a); (c) Hilbert envelope spectrum of (b); and (d) zoom-in view of (b) in which two sets of periodic impulses are observed.

Recalling the fault characteristic frequency for outer race BPFO = 83.3Hz, the sampling points during one fault period is $T_{s2} = f_s/BPFO = 120$. $WCK_1(t,T_{s2})$ is calculated from the filtered signal and displayed in Fig. 6(b), which provides periodic pulses as the insert picture shows. Fig. 6(c) provides the Hilbert envelope spectrum of $WCK_1(t,T_{s2})$. It is seen that the fundamental and harmonics of $X_2 = 83.7\text{Hz}$ which is very close to BPFO are the primary frequency components. Thus,

$WCK_1(t,T_{s2})$ isolated the periodic, outer race defect impulses from the filtered signals. To identify the defects number, a zoom-in view of $WCK_1(t,T_{s2})$ is displayed in Fig. 6(d). The circles, diamonds, and pentagons denote three sets of periodic impulses whose period corresponds to BPFO, indicating that there exist three localized outer race damages on the tested baring. Also, the strengths of the three impulses sets are different, resulting from the different defect sizes and locations in different load areas.

Considering the detection of the roller damages, the filtered signal in the third subband decomposed by the optimal FAWT basis $B_{3,4,9,10}$ is shown in Fig. 7(a). The sampling points during one fault period of the rollers are calculated as $T_{s1} = f_s/BPF = 149$, based on which the WCK is estimated and exhibited in Fig. 7(b). It is clear that the $WCK_1(t,T_{s1})$ is pure periodic pulses whose period corresponds to BPF, as validated via its Hilbert envelope spectrum shown in Fig. 7(c). Also, it reveals that $WCK_1(t,T_{s1})$ effectively isolated the roller defect signature from the filtered signals. It is found $WCK_1(t,T_{s1})$ also contains alternative impulses and noise zones. To clearly identify the defects number, the zoom-in view of $WCK_1(t,T_{s1})$ during one impulses zone is displayed in Fig. 7(d). Two successive sets of periodic impulses are existed in the impulses zone, indicating two local defects on the rollers. Thus, the experiment data analysis validates that WCK algorithm could isolate interested periodic fault impulses effectively.

IV. Conclusion

This paper proposes a technique for isolating compound faults and identifying defects number from the vibration measurements of locomotive bearings. The technique mainly contains two steps: filtering; and faults isolation and identification. During the raw vibration signals filtering, FAWT possessing arbitrary and flexible time-frequency partition property is adopted to adaptively denoise the vibration signals. When the filtered signals are achieved, the faults isolation and identification via the WCK are post-processing procedures which work on the filtered signals. WCK greatly enhances the interested periodic faults via effectively eliminating the noise and other fault modes. The fault signature can be further captured from the Hilbert envelope spectrum as the fundamental and harmonics of the fault characteristic frequency. The proposed technique is tested via experimental measurements. It is validated that WCK can effectively isolate compound faults sharing the same characteristic frequency from different bearing components, and the faults number can be determined via counting the interested periodic pulses in the WCK outputs.

Acknowledgment

Great acknowledgement is made to the editors and reviewers for the constructive and valuable comments which help us a lot in improving the manuscript quality.

References

[1] Z. Zhao, S. Wu, B. Qiao, S. Wang, and X. Chen, “Enhanced sparse period-group lasso for bearing fault diagnosis,” IEEE T. Ind. Electron., vol. 66, no. 3, pp. 2143-2153, 2019.

[2] C. Zhang, B. Li, B. Chen, H. Cao, Y. Zi, Z. He, “Weak fault signature extraction of rotating machinery using flexible analytical wavelet transform,” Mech. Syst. Signal Pr., vol. 64-65, pp. 162-187, 2015.

[3] T. Wang, F. Chu, and Z. Feng, “Meshing frequency modulation (MFM) index-based kurtogram for planet bearing fault detection,” J. Sound Vib., vol. 432, pp. 437-453, 2018.

[4] L. Niu, H. Cao, Z. He, and Y. Li, "Dynamic Modeling and Vibration Response Simulation for High Speed Rolling Ball Bearings With Localized Surface Defects in Raceways," J. Manuf. Sci. E.-T. ASME., vol. 136, no. 4, 2014.

[5] H. Jiang, J. Chen, and G. Dong, “Hidden Markov model and nuisance attribute projection based bearing performance degradation assessment,” Mech. Syst. Signal Pr., vol. 72-73, pp. 184-205, 2016.

[6] Y. Li, Y. Yang, X. Wang, B. Liu, and X. Liang, “Early fault diagnosis of rolling bearings based on hierachical symbol dynamic entropy and binary tree support vector machine,” J. Sound Vib., vol. 428, pp. 72-86, 2018.

[7] Y. Lei, J. Lin, Z. He, and M.J. Zuo, “A review on empirical mode decomposition in fault diagnosis of rotating machinery,” Mech. Syst. Signal Pr., vol. 35, no. 1-2, pp. 108-126, 2013.

[8] Y. Miao, M. Zhao, J. Lin, and Y. Lei, “Application of an improved maximum correlated kurtosis deconvolution method for fault diagnosis of rolling element bearings,” Mech. Syst. Signal Pr., vol. 92, pp. 173-195, 2017.

[9] H. Wang, R. Li, G. Tang, H. Yuan, Q. Zhao, and X. Cao, “A compound fault diagnosis for rolling bearings method based on blind source separation and ensemble empirical mode decomposition,” Plos One, vol. 9, no. 10, p. e109166, 2014.

[10] Y. Hao, L. Song, Y. Ke, H. Wang, and P. Chen, “Diagnosis of compound fault using sparsity promoted-based sparse component analysis,” Sensors, vol. 1307, p. s17061307, 2017.

[11] Y. Jiang, H. Zhu, and Z. Li, “A new compound faults detection method for rolling bearings based on empirical wavelet transform and chaotic oscillator,” Chaos, Solitons Fract., vol. 89, pp. 8-19, 2016.

[12] W. Fan, Q. Zhou, J. Li, and Z. Zhu, “A wavelet-based statistical approach for monitoring and diagnosis of compound faults with application to rolling bearings,” IEEE T. Autom. Sci. Eng., vol. 15, no. 4, pp. 1563-1572, 2018.

[13] X. Gu, S. Yang, Y. Liu, F. Deng, and B. Ren, “Compound faults detection of the rolling element bearing based on the optimal complex Morlet wavelet filter,” P. I. Mech. Eng. C.-J. Mec., vol. 232, no. 10, pp. 1786-1801, 2018.

[14] C. Zhang, Y. Liu, F. Wan, B. Chen, J. Liu, and B. Hu, "Multi-faults diagnosis of rolling bearings via adaptive customization of flexible analytical wavelet bases," Chinese J. Aeronaut., 2019. DOI: 10.1016/j.cja.2019.03.014.

[15] C. Zhang, Y. Liu, F. Wan, B. Chen, and J. Liu, "Isolation and Identification of Compound Faults in Rotating Machinery via Adaptive Deep Filtering Technique," IEEE Access, vol. 7, pp. 139118-139130, 2019.

[16] D. He, X. Wang, S. Li, J. Lin, and M. Zhao, “Identification of multiple faults in rotating machinery based on minimum entropy deconvolution combined with dpectrum kurtosis,” Mech. Syst. Signal Pr., vol. 81, pp. 235-249, 2016.

[17] Z. Yi, N. Pan, and Y. Guo, “Mechanical compound faults extraction based on improved frequency domain blind deconvolution algorithm,” Mech. Syst. Signal Pr., vol. 113, pp. 180-188, 2018.

[18] G. McDonald, Q. Zhao, and M.J. Zuo, “Maximum correlated Kurtosis deconvolution and application on gear tooth chip fault detection,” Mech. Syst. Signal Pr., vol. 33, pp. 237-255, 2012.